Journal of the Mechanics and Physics of Solids 63 (2014) 187–200

Contents lists available at ScienceDirect

Journal of the Mechanics and Physics of Solids

journal homepage: www.elsevier.com/locate/jmps

Theory of cyclic creep of concrete based on Paris law for fatigue growth of subcritical microcracks

Zdenek P. Bazant [a,*], Mija H. Hubler [b]

[a] Civil and Mechanical Engineering, and Materials Science, Northwestern University, 2145 Sheridan Road, CEE/A135, Evanston, IL 60208, United States

[b] Civil and Environmental Engineering, Massachusetts Institute of Technology, 77 Massachusetts Ave., 1-290, Cambridge, MA 02139, United States

ARTICLE INFO

Article history:
Received 11 July 2013
Received in revised form
9 September 2013
Accepted 14 September 2013
Available online 2 October 2013

Keywords:
Concrete
Cyclic creep
Microcracks
Paris law

ABSTRACT

Recent investigations prompted by a disaster in Palau revealed that worldwide there are 69 long-span segmental prestressed-concrete box-girder bridges that suffered excessive multi-decade deflections, while many more surely exist. Although the excessive deflections were shown to be caused mainly by obsolescence of design recommendations or codes for static creep, some engineers suspect that cyclic creep might have been a significant additional cause. Many investigators explored the cyclic creep of concrete experimentally, but a rational mathematical model that would be anchored in the microstructure and would allow extrapolation to a 100-year lifetime is lacking. Here it is assumed that the cause of cyclic creep is the fatigue growth of pre-existing microcracks in hydrated cement. The resulting macroscopic strain is calculated by applying fracture mechanics to the microcracks considered as either tensile or, in the form of a crushing band, as compressive. This leads to a mathematical model for cyclic creep in compression, which is verified and calibrated by laboratory test data from the literature. The cyclic creep is shown to be proportional to the time average of stress and to the 4th power of the ratio of the stress amplitude to material strength. The power of 4 is supported by the recent finding that, on the atomistic scale, the Paris law should have the exponent of 2 and that the exponent must increase due to scale bridging. Exponent 4 implies that cyclic creep deflections are enormously sensitive to the relative amplitude of the applied cyclic stress. Calculations of the effects of cyclic creep in six segmental prestressed concrete box girders indicate that, because of self-weight dominance, the effect on deflections absolutely negligible for large spans (>150 m). For small spans (<40 m) the cyclic creep deflections are not negligible but do not matter since the static creep causes in such bridges upward deflections. However, the cyclic creep is shown to cause in bridges with medium and small spans (<80 m) a significant residual tensile strain which can produce deleterious tensile cracking at top or bottom face of the girder.

1. Introduction

A segmental prestressed-concrete box-girder bridge built in 1977 in Palau, which had the world record span of 241 m, deflected within 18 years by 1.61 m. This was 5.3-times greater than the allowable deflection. An attempt to lift the midspan

* Corresponding author. Tel.: +1 847 491 4025; fax: +1 847 491 4011.
E-mail address: z-bazant@northwestern.edu (Z.P. Bazant).

0022-5096/$ - see front matter © 2013 Elsevier Ltd. All rights reserved.
http://dx.doi.org/10.1016/j.jmps.2013.09.010

by additional prestressing led three month later to collapse (with fatalities). Subsequent worldwide search for data (Bazant et al., 2011a) revealed that 69 large-span bridges of the same type suffered within 20–40 years long-time deflections most of which are excessive and require either replacement of the bridge or risky remedial prestressing. Although a detailed analysis (Bazant et al., 2012a, 2012b) showed that these excessive deflections can be explained by severe underestimation of multidecade (static) creep of concrete in the current design codes and standard recommendations (ACI Committee 209, 1972, 2008; FIB, 1999; Gardner, 2000; Gardner and Lockman, 2001; Bazant and Baweja, 1995, 2000), some engineers at conferences questioned whether the cyclic creep due to traffic loads may have been a significant contributing factor. Examination of this question was the motivation for the present study in which a constitutive law for cyclic creep is developed and calibrated by the available test data.

The cyclic creep of concrete, also called the fatigue creep or vibro-creep (vibropolzuchest' in Russian), is the long-time deformation produced by cyclic load in excess of the static creep. This phenomenon was experimentally detected by Féret in 1906 and was also observed by Probst in 1925, Mehmel and Heim in 1926, and Ban in 1933 (cf. Bechyně, 1959). More systematic experiments that allow quantitative characterization had to wait until the works of Kern and Mehmel (1962) and Gaede (1962). After World Word II, many researchers studied this phenomenon experimentally and proposed various approximate empirical formulas (Le Camus, 1946; L'Hermite, 1961; Mal'mejster, 1957; L'Hermite, 1961; Murdock, 1965; Gvozdev, 1966; Bennett and Muir, 1967; Nordby, 1967; Bazant, 1968a, 1968b; Batson et al., 1972; Wittmann, 1971; Whaley and Neville, 1973; Hirst and Neville, 1977; Neville and Hirst, 1978; Bazant and Panula, 1979; Garrett et al., 1979; Hsu, 1981; Brooks and Forsyth, 1986; Bazant et al., 1992; Pandolfi and Taliercio, 1998). Yet mutually contradictory formulations abound and no generally accepted theory has yet emerged.

In 1962, Gaede (1962) proposed the following formula based on his own extensive tests of cyclic compression:

$$\Delta\varepsilon_N = \frac{cN_0}{f_p}\frac{\sigma_{max}}{E_{sec}}\left(\frac{N}{N_0}\right)^r \tag{1}$$

where $\Delta\varepsilon_N$ = strain increment due to cyclic loading; N = number of cycles, $N_0 = 10^5$; f_p = compressive strength of prisms; c and r = empirical fitting parameters with no mechanical explanation provided; and E_{sec} = instantaneous elastic modulus measured for pulsating compression. Eq. (1) was based on compression cycles from 14% to 75% of the compression strength f'_c, which is way beyond the service stress range allowed in bridge design ($< 40\%$ of f'_c).

Wittmann (1971) tried to generalized his power law for a (static) creep curve, $\varepsilon(t) = at^n \sinh(b\sigma/f_c)$ in which a, b are empirical constants. The aging effect was ignored, and a hyperbolic sine function ensued from an assumption of thermally activated transitions. Considering cyclic stress $\sigma = \sigma_m + \Delta\sigma \sin \omega t$ where ω = constant and $\sigma_m, \Delta\sigma$ = the mean and amplitude of cyclic stress, he empirically generalized this power law by replacing the constant exponent n with the variable $n = n_0 + c(\Delta\sigma/f_c)^d$ where n_0, c, d are constants which he calibrated by Gaede's data.

Hirst and Neville (1977), Neville and Hirst (1978) and Whaley and Neville (1973) presented the most comprehensive and diverse experimental data. In Neville and Hirst (1978), they proposed that the cyclic creep is an inelastic deformation caused by microcracking, but made no attempt to model the microcracking per se. In view of the hardening effect under low stress cyclic creep observed in some experiments (Bennett and Muir, 1967; Hirst and Neville, 1977; Neville and Hirst, 1978; Whaley and Neville, 1973; Batson et al., 1972), they suggested that the microcracking occurs at the aggregate interfaces. Garrett and Jennings, Garrett et al. (1979), speculated that these microcracks could expose unhydrated cement to further hydration which in turn might cause further deformation. Hirst, and later also Brooks Hirst and Neville (1977); Brooks and Forsyth (1986), assumed that $\varepsilon_{\text{cyclic}} = \varepsilon_{\text{static}} A(\ln t)^B$, where ε is the creep strain and A, B are calibration parameters.

Later on, Pandolfi and Taliercio (1998) suggested a more complicated formula for cyclic creep of concrete based on numerical simulations. They emphasized two concepts: The time is only implicitly related to the number of cycles, N, i.e., the tests should be interpreted in terms of N, the number of cycles, and the loading frequency is indirectly related to the loading rate (Hsu, 1981). Damage evolution models based on failure surfaces in the stress space have also been suggested. It appears, however, that no model based on fatigue growth of individual microcracks under cyclic loading has been presented.

The phenomenological formulations treated cyclic creep in two ways: either as a deformation $\Delta\varepsilon_N$ that is additional to the static creep (Bazant, 1968a) or as an acceleration of the static creep (Bazant and Panula, 1979; Bazant et al., 1992, 2012b). Both were able to provide acceptable fit of the main data, doubtless because of their limited duration (mostly < 10 days, some up to 28 days). However, extrapolations to lifetimes of up to 100 or 150 years, usually desired for large bridges, give very different predictions.

In this paper, a micro-mechanical model for cyclic creep is proposed and calibrated by tests. Although the micro-mechanics has been discussed intuitively in qualitative terms (e.g., Neville and Hirst, 1978; Garrett et al., 1979) or in terms of phenomenological damage mechanics (Gao and Hsu, 1998; Maekawa and El-Kashif, 2013), no micro-mechanics based and experimentally validated constitutive model seems to have been proposed during a century of research. This is what the present study aspires to.

2. What is the microscale mechanism?

In fatigue embrittled metals or in fine-grained ceramics, a critical safety consideration is the fatigue growth of cracks. Although such dangerous cracks can be small, they are nevertheless macrocracks because they are larger than the

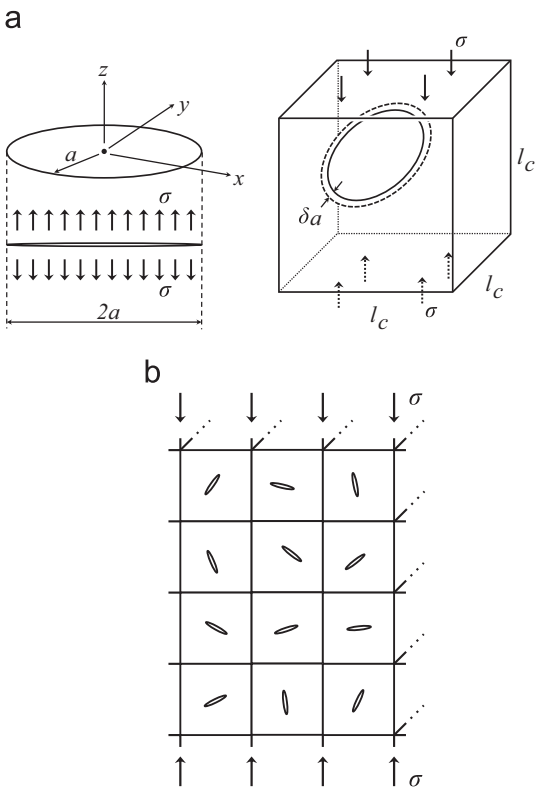

Fig. 1. (a) Generic microcrack in three dimensions, and a mode I penny-shaped crack; (b) set of sparse microcracks and crushing bands, one in each cube of side l_c.

representative volume element (RVE) of the material. In contrast to concrete, these materials are relatively homogeneous from micrometer scale up.

Unlike metals and fine-grained ceramics, the microstucture of concrete is disordered on all the scales, from the nanoscale to the macroscale of an RVE, whose size is typically 0.1 m (assuming normal size aggregates). On all scales, the material is full of flaws and preexisting cracks. The growth of cracks larger than the RVE is blocked by reinforcing bars, and cracks much smaller than the RVE are not important for safety. Under fatigue loading, such cracks must be expected to grow but affect only inelastic deformation rather than safety since they are much smaller than the RVE. Indeed, the experimental results for cyclic compressive loading of concrete within the service stress range (i.e., for stresses less than 40% of the strength) indicate no degradation of material strength for subsequent short-time loading up to failure and only a slight decrease of concrete stiffness (Hellesland and Green, 1971).

3. Macroscopic strain due to small growth of microcracks

Consider a generic three-dimensional planar macrocrack of size a (denoting, e.g., the radius of a penny-shaped crack); Fig. 1a. In the case of compression loading, a shear crack with a combination of modes II and III is relevant, and in the case of tensile loading, a mode I crack. For the sake of simplicity, the crack is assumed to grow in a self-similar way, expanding in its plane in proportion to a. The energy release rate due to three-dimensional self-similar growth of the crack may generally be expressed as

$$\mathcal{G}=\frac{\gamma_1}{a}\left[\frac{\partial \Pi^*}{\partial a}\right]_\sigma \tag{2}$$

where Π^* is the complementary energy (or Gibbs' free energy) per microcrack, σ=applied remote stress, and γ_1=dimensionless geometry factor which, e.g., would be equal to $1/\pi$ in the case of a penny-shaped crack in mode I. Even though K_I, K_{II}, K_{III} must vary along the crack edge in three dimensions, one can define an effective stress intensity factor at the crack edge on the basis of the average energy release rate of the microcrack, i.e.,

$$K=\sqrt{E\mathcal{G}} \tag{3}$$

where, in general,

$$\mathcal{G}=\gamma_2 a\sigma^2/E \tag{4}$$

Here E=Young's elastic modulus and γ_2=dimensionless geometry factor. For the simple case of a mode I penny-shaped crack, $K=K_I=2\sigma\sqrt{a/\pi}$ (Tada et al., 1973), which gives $\gamma_2=4/\pi$.

According to Eqs. (2) and (4), the total energy release rate of the crack is

$$\left[\frac{\partial \Pi^*}{\partial a}\right]_\sigma = \frac{\gamma_2\sigma^2}{\gamma_1 E}\,a^2 \tag{5}$$

Integrating at constant σ, one gets

$$\Pi^* = \frac{\gamma_2\sigma^2}{3\gamma_1 E}\,a^3 \tag{6}$$

Let the volume per microcrack be l_c^3 and consider, for the sake of simplicity, all the microcracks to be normal to the direction of applied stress σ. According to Castigliano's theorem (see, e.g., Castigliano, 1873 or Flügge, 1962), we may calculate the displacement u per crack as follows:

$$u=\left[\frac{\partial \Pi^*}{\partial P}\right]_a=\frac{1}{l_c^2}\left[\frac{\partial \Pi^*}{\partial \sigma}\right]_a=\frac{\gamma_0}{El_c^2}\sigma a^3 \tag{7}$$

where $P=\sigma l_c^2$, the applied force per crack, and the notation $\gamma_0=2\gamma_2/3\gamma_1$ is a dimensionless constant characterizing the geometry. Since $u=l_c\varepsilon$, the macroscopic strain caused by the formation of microcracks of size a under remotely applied stress σ is $\varepsilon=u/l_c$ or

$$\varepsilon=\frac{\gamma_0}{El_c^3}\,\sigma a^3 \tag{8}$$

The total microcrack size increment over N cycles is $\Delta a_N=a_N-a_0$ where a_N is the crack size after N cycles and a_0 is the initial crack size before cyclic loading. According to Eq. (8), the strain increment due to cyclic loading is

$$\Delta\varepsilon_N=\frac{\gamma_0}{El_c^3}\,\sigma\left(a_N^3-a_0^3\right)=\frac{\gamma_0}{El_c^3}\,\sigma a_0^3\left[\left(1+\frac{\Delta a_N}{a_0}\right)^3-1\right] \tag{9}$$

In failure analysis, large Δa_N need to be considered. But since the creep strains in service are always small, we may assume that $\Delta a_N/a_0 \ll 1$. Noting that $(1+x)^3\approx 1+3x$ when $x\ll 1$, Eq. (9) may thus be linearised as follows:

$$\Delta\varepsilon_N=3\gamma_0\,\frac{\sigma}{E}\left(\frac{a_0}{l_c}\right)^3\frac{\Delta a_N}{a_0} \tag{10}$$

4. Paris law and strain due to subcritical growth of microcracks

Consider cyclic loading of amplitude $\Delta\sigma=\sigma_{max}-\sigma_{min}$ (Fig. 1c). Paris (with Erdogan) (Paris and Erdogan, 1963) showed that, except for very large stress amplitudes and very high σ_{max} occurring in failure analysis, the fatigue growth of a crack depends only on the amplitude ΔK of the stress intensity factor K but not on its maximum and minimum individually. So the Paris law reads

$$\frac{\Delta a}{\Delta N}=\lambda\left(\frac{\Delta K}{K_c}\right)^m \tag{11}$$

where K_c is the critical stress intensity factor for monotonic loading. Prefactor $\lambda$and exponent m are empirical constants. The Paris Law is a good approximation for the intermediate range of fatigue crack growth, which is relevant for creep deflections of structures in service. For very large or small ΔK, the crack growth rate deviates from the slope m, producing a S-shaped deviations when K_{max} and ΔK exceed certain thresholds ΔK. While exceeding these thresholds is important for failure analysis, it is not for deformations in the service stress range (i.e., for stresses less than 40% of the strength limit). When the K_{max} and *Del K* vary broadly, it is further important to take into account the dependence of prefactor λon the ratio $R=K_{max}/K_{min}$, but again this is not important within the service stress range. Recently it has been shown that on the atomic scale, exponent m must be equal to 2 and that m must increase when moving up to higher scales (Bazant and Le, 2009; Le and Bazant, 2011).

For mode I microcracks, the K should be interpreted as K_I, the mode I stress intensity factor. But for shear cracks and compressive loading, K should be understood as a certain effective value of a combination of mode II and mode III stress intensity factors along the crack front edge in three dimensions, and may better be interpreted as a characteristic derived from the average energy release rate, $\mathcal{G}=K^2/E$, along the crack edge.

For polycrytalline metals, for which the fracture process zone (FPZ) size is on the micrometer scale, exponent m is known to be around 4 (Kanninen and Popelar, 1985), while for the macrocracks in concrete m is about 10 (Bazant and Xu, 1991) and in ceramics about 30. The increase seems to be explained by the recent finding that the exponent of the Paris law must grow when moving up through the scales in material (Le and Bazant, 2011). In concrete, the FPZ size is of the order of 0.1 m. Unlike metals and ceramics, for macrocracks in concrete the prefactor λ was found to depend on the structure size (Bazant

and Xu, 1991; Baănt and Schell, 1993), which was shown to be caused by a non-negligible size of the FPZ compared to the structure size. But here the λ cannot depend on the structure since we consider only microcracks far smaller than the FPZ.

The amplitude ΔK is proportional to the remotely applied stress amplitude $\Delta\sigma$, i.e.,

$$\Delta K = c\sqrt{a}\Delta\sigma \tag{12}$$

where c is a dimensionless geometry constant. E.g., for mode I penny shaped cracks, $c = 2/\sqrt{\pi}$. Substituting Eq. (12) into (11), we would get variable a on both sides of the equation. Although the resulting differential equation could be easily integrated by parts, we may consider that, in the case of creep under service loads, $\Delta a \ll a_0$. So, $\Delta K = c\sqrt{a_0}\Delta\sigma$. Integration at constant $\Delta\sigma$ then furnishes, for small crack extensions:

$$a_N - a_0 = \lambda\left(\frac{c\Delta\sigma\sqrt{a_0}}{K_c}\right)^m N \tag{13}$$

5. Cyclic creep formula ensuing from Paris law

Substituting Eq. (13) into (10) and rearranging, we obtain for the strain increment due to cyclic creep after N cycles the formula:

$$\varepsilon_N = C_1\,\sigma\left(\frac{\Delta\sigma}{f'_c}\right)^m N \tag{14}$$

$$\text{where } C_1 = \frac{3\gamma_0}{E}\frac{\lambda}{a_0}\left(\frac{ca_0}{l_c}\right)^3\left(\frac{f'_c\sqrt{a_0}}{K_c}\right)^m \tag{15}$$

Here f'_c is the standard compression strength of concrete, introduced merely for convenience of dimensionality.

It is noteworthy that ε_N is predicted to depend on both σ and N linearly. This agrees with the available cyclic creep measurements and is convenient for structural analysis.

6. Quantitative estimates

Let us now use Eq. (10) to estimate the magnitude of $\Delta a_N/a_N$. This can be done easily for mode I penny-shaped cracks. According to the aforementioned values of γ_1 and γ_2 for penny-shaped cracks, we have $\gamma_0 = 2\gamma_2/3\gamma_1 = 2(4/\pi)/(3\pi) = 8$. The ratio $\varepsilon_{el} = \sigma/E$ represents the elastic strain under the static stress component. The ratio $\Delta\varepsilon_N/\varepsilon_{el}$ may, according to experiments, reach about 0.05.

To calculate the macroscopic strain, one simple possibility is to idealise the microcracks as nearly dilute (i.e., approximately non-interacting), in which case E would be the Young's modulus of the uncracked matrix and the size l_c of the cubical material domain per microcrack would have to be at least 3-times larger than the crack size, a_0, i.e., $l_c/a_c \approx 3$. Then Eq. (10) would indicate that

$$\Delta a_N/a_0 = 0.05 \times 27/(8/3) \approx 0.51 \tag{16}$$

This value is certainly not small enough to make the linearisation of Eq. (9) accurate.

Another simple possibility is to assume that the microcracks are very dense. In that case, following the classical philosophy of Eschelby, one microcrack may be assumed to be embedded in a homogeneous elastic continuum in which E represents the effective or average macroscopic properties of the microcracked material. Considering that, e.g., $l_c \approx a_0$, Eq. (17) is now replaced by

$$\Delta a_N/a_0 = 0.05/(8/3) \approx 0.019 \tag{17}$$

Concrete, or cement hydrate, is known to be full of microcracks. So, the second possibility, Eq. (17) for dense microcracks, is more realistic. This means we can use the linearisation in Eq. (9). At the same time, it should be noticed that Eq. (14) obtained upon linearisation does fit well the cyclic creep data for the service stress range.

7. Dimensional analysis and similitude: compressive cyclic loading

Although the analysis in Eqs. (2)–(9) was exemplified by a mode I crack, it is equally applicable to cyclic creep under compressive and shear loadings, which are of main practical interest for prestressed structures in which almost no concrete is under tension. Under compression, five types of cracks producing inelastic compressive strain can be distinguished:

(a) crushing band propagating transversely to compression (Suresh, 1998; Suresh et al., 1989; Eliáš and Le, 2012, p.193) (Fig. 3a);
(b) wedge-splitting cracks (Bazant and Xiang, 1997) at hard inclusions, parallel to compression (Fig. 3b);
(c) interface cracks at inclusions (Fig. 3c);

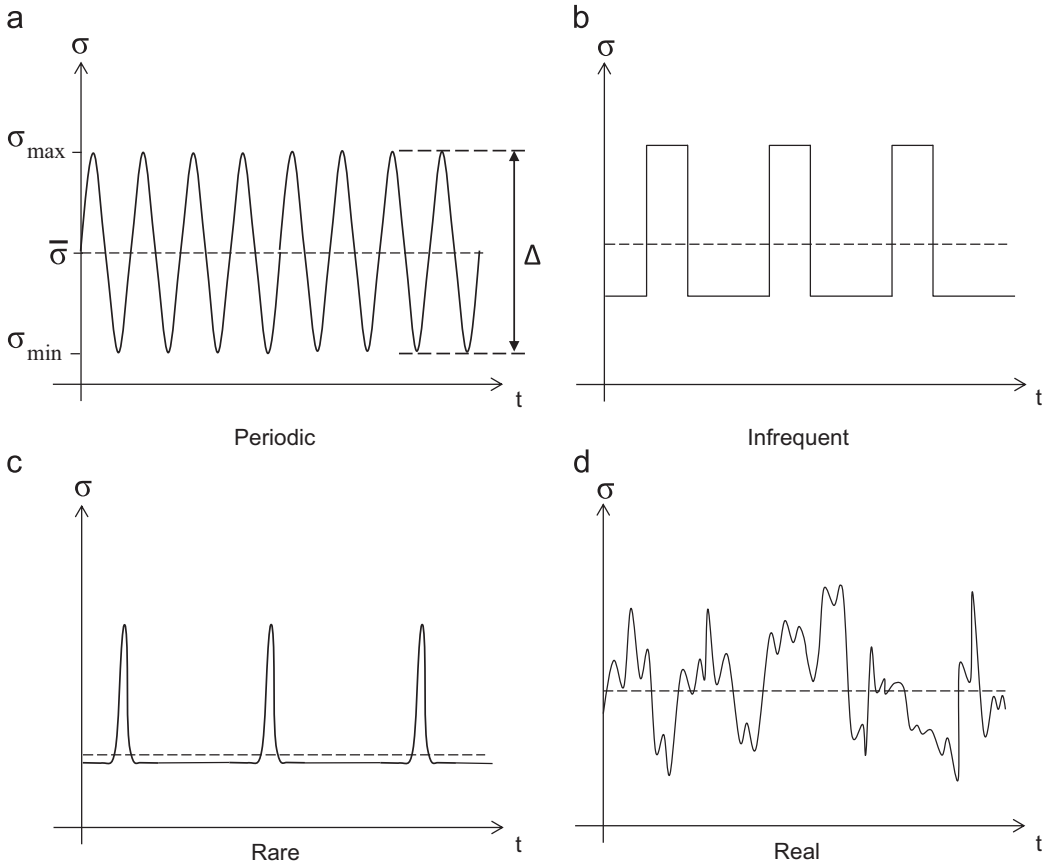

Fig. 2. Typical cyclic stress histories: (a) periodic loading, (b) infrequent cycles, (c) rare cycles, and (d) real loading.

(d) pore-opening cracks parallel to compression (Sammis and Ashby, 1986; , Fairhurst and Comet, 1981) (Fig. 3d); and
(e) wing-tip frictional cracks inclined to compression direction (Ashby and Hallam, 1986; Horii and Nemat-Nasser, 1982; Ingraffea, 1977; Kachanov, 1982; Schulson and Nickolayev, 1995) (Fig. 3e).

The last is observed only rarely and is the only type that can be conceived to develop in a homogeneous medium that contains only preexisting microcracks or weak planes but neither inclusions nor pores (Schulson and Nickolayev, 1995). The first type, i.e., Suresh's crack growth, differs from the others in that only a finite crack extension is possible, but in the present case it does not matter since very small crack length growth is assumed at the outset.

Detailed mathematical analysis of these compressive cracks would be rather complicated. We will, therefore, resort to dimensional analysis and similitude considerations (Barenblatt, 1979, 2003). According to Buckingham's Π-theorem (Buckingham, 1914; Barenblatt, 1979) (which should in fairness be called the Vashy–Buckingham theorem (Vashy, 1892)), the number of independent governing parameters $N=N_t-N_d$ where N_t is the total number of governing parameters and N_d is the number of independent physical dimensions among the parameters.

In the equation for energy release rate, Eq. (4), from which everything follows, the independent parameters are crack size a [dimension m], applied remote stress σ[dimension N/m^2], elastic modulus E [dimension N/m^2], and the energy release rate per unit area of crack $\mathcal{G}$ [dimension N/m]. Here we have only two independent dimensions, length and force. So the number of dimensionless independent parameters is $N=4-2=2$. They can be selected as

$$\Pi_1=\frac{E\mathcal{G}}{\sigma^2 a},\ \Pi_2=\frac{\sigma}{E} \tag{18}$$

where $K^2=E\mathcal{G}$. The governing relation must have the form $\Phi(\Pi_1,\Pi_2)=0$, and since, in the special case of mode I penny-shaped crack, the governing relation must coincide with Eq. (5), it must have the form $\Pi_1-\mu_0\Pi_2=0$ where μ_0 is a constant. Indeed, this gives

$$\mathcal{G}=\mu_0\frac{\sigma^2}{E}a^2 \tag{19}$$

which is identical to Eq. (5) (with $\mu_0=\gamma_2/\gamma_1$). The subsequent derivation of the cyclic creep strain proceeds the same way as before, i.e., the integration of (19) at constant load yields the complementary energy, whose differentiation at constant

length then yields (according to Castigliano's theorem) the displacement. This is then combined with the Paris law and leads to the same form of the cyclic creep law. Although the Paris law seems not to have been tested for cyclic compression (except for transverse crushing band (Suresh, 1998)), it is expected to apply.

8. Cyclic creep compliance and multi-axial generalisation

Because σ appears in Eq. (14) linearly, it is possible to define the cyclic creep compliance $\Delta J_N = \Delta\varepsilon_N/\sigma$, i.e.,

$$\Delta J_N = C_1 \left(\frac{\Delta\sigma}{f_c'}\right)^m N \tag{20}$$

The total material compliance in presence of cyclic loading component is

$$J_{tot} = J(t,t') + \Delta J_N \tag{21}$$

where $J(t,t')$ is the compliance for creep (including elastic response), as given, e.g., by model B3 (Bazant and Baweja, 2000). It is defined as the strain at time t caused by a unit applied uniaxial stress introduced at concrete age t'. However, the linear engineering theory of bending cannot be used, since the distribution of $\Delta\sigma$ over the cross section is nonlinear and thus makes the distribution of ε_N over the cross section nonlinear (cf. Bazant, 1968a).

No experimental information seems to exist for cyclic creep under multi-axial stress or tensile loading, nor cyclic creep with cycles of varying amplitudes. Nevertheless it appears reasonable to neglect transverse strains and to expect that under tension the cyclic creep per unit stress is at least as large as it is under compression. Also note that, for the special case of a crack normal to the principal stress, an analysis similar to Eqs. (2)–(8) gives a zero lateral strain.

A three-dimensional finite element program for creep and cyclic creep in a bridge has been formulated in Bazant et al. (2012b) under the assumption that the cyclic creep eigenstrains corresponding to individual principal stresses can be superposed.

9. Simpler alternative of limited applicability: time acceleration

Within a time interval in which the compliance rate $\dot{J} = \partial J(t,t')/\partial t$ is nearly constant, it is alternatively also possible to model the cyclic creep as an acceleration of the static creep obtained upon increasing the creep duration by $\Delta t_N = J_N \Delta(\ln J_N)/\dot{J}_N$, which is

$$\Delta t_N = C_t \left(\frac{\Delta\sigma}{f_c'}\right)^m N \text{ where } C_t = C_1 \frac{\Delta(\ln J_N)}{\dot{J}_N} \tag{22}$$

Formulating the cyclic creep as an acceleration of static creep is simple and computationally convenient, but is acceptable only for limited time intervals. The reason that the existing test data could be fitted in this manner also well (Bazant and Panula, 1979; Bazant et al., 1992) is that the data duration is very limited (only about 10 days) and is such that parameter C_t in the last equation does not change much within the time span of the data.

However, for a general creep prediction model covering multi-decade structural response, $\dot{J}$ cannot be assumed to be constant. So the cyclic creep must be considered to be an eigen-strain, as written in Eq. (21) (which is the way the cyclic creep was empirically treated in Bazant (1968a, 1968b)). In extrapolation to the structural lifetimes of 20–150 years, this makes an enormous difference.

10. Calibration by fitting of existing test data

Experimental verification relied on well-documented laboratory data from the literature. Because the present analysis applies only to cyclic creep under service stresses, which are generally limited to less than 40% of concrete strength, the tests in which this limit was exceeded, or in which fatigue failure occurred, have not been considered. For each curve, the B3 creep model (Bazant and Baweja, 2000) was first calibrated to fit the static creep curve (i.e., curve for zero stress amplitude), which must be subtracted from the data to separate the effect of cyclic creep. The B3 parameters thus calibrated were then used in the joint least-square optimization of the fit of all cyclic test curves to determine optimum cyclic creep parameters C_t and m in Eq. (20). The fits of the test curves are shown in Fig. 4. They include both cyclic creep and static creep, the latter under either sealed conditions (basic creep) or drying conditions (drying creep).

The data set of Whaley and Neville (1973) is the most comprehensive set available, containing cyclic tests done under both sealed and drying conditions. The initial strains, which were not reported, were estimated by extrapolation of the model B3 curve fitted to the initial portion of the data. Whaley and Neville measured the cyclic creep at various amplitudes and mean stress levels, at a frequency of 585 cycles/min. One of their data sets, studying the effect of mean stress, could not be used because the maximum stresses in the cycles exceeded the fatigue limit. Also considered were the tests of Kern and Mehmel (1962) with co-workers, which reported the effect of stress cycling on the drying creep at various average stresses and various amplitudes of the cyclic load, at two different frequencies, 380 cycles/min and 3000 cycles/min. Furthermore, Hirst and Neville (1977) reported tests at 3000 cycles/min and various stress amplitudes. Further cyclic test data do exist,

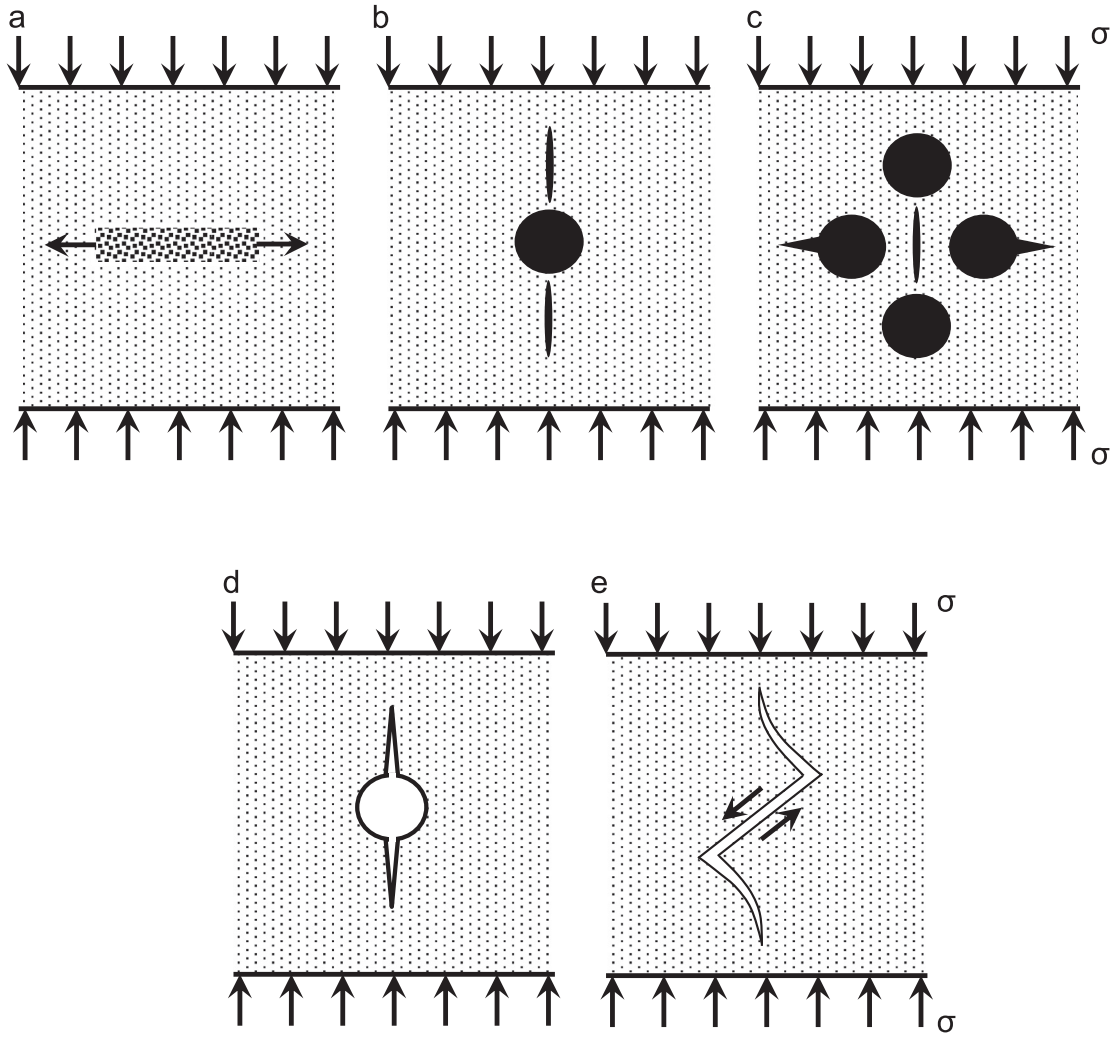

Fig. 3. Five types of cracks producing axial inelastic strain; (a) transversely propagating crushing band, (b) axial wedge-splitting cracks at hard inclusions in hardened cement paste, (c) interface cracks at inclusions, (d) pore-opening axial cracks, and (e) inclined wing-tipped frictional cracks.

but were not used because they either lacked the reference static creep test (at zero amplitude) or used a concrete with unusual mix proportions beyond the scope of model B3.

The calibrated fit of Eq. (20) to the test data is presented in Fig. 4. With the optimized parameter values $C_t = 46 \times 10^{-6}$ and $m = 4$, all the data were fitted with a coefficient of variation of only 0.05 (root-mean-square error divided by data mean).

The fact that the experiments verify the exponent value $m = 4$ is interesting. According to the activation energy based probabilistic theory of quasibrittle fracture (Bazant and Le, 2009; Le and Bazant, 2011), exponent m of the Paris law should be equal to 2 on the nano-scale. Moving up through the scales causes the exponent m of the crack growth law to increase by approximately 2 for each order of scale magnitude. This matches the fact that for metals and fine-grained ceramics, in which the RVE is of micrometer size, $m \approx 4$. In concrete, one has to cross several more scales to reach the scale of an RVE, which is of the size of 0.1 m. Thus it is not surprising that the exponent of Paris law of for macroscale crack propagation in concrete is about 10 (Bazant and Xu, 1991). In this light, it is not at all surprising that the cyclic creep exponent of concrete is equal to 4. In view of the theory of Bazant and Le, this value of m implies that the relevant cracks that cause the cyclic creep should be micrometer scale cracks, far smaller than the RVE size. Thus we have a partial theoretical support for our starting hypothesis.

11. Estimate of magnitude of cyclic creep effects in structures

Let us now consider prestressed segmental box girders, which are very efficient structures for bridges of spans from 40 m to 250 m. However, It has not been widely realized that they are prone to excessive multi- decade creep deflections (Bazant

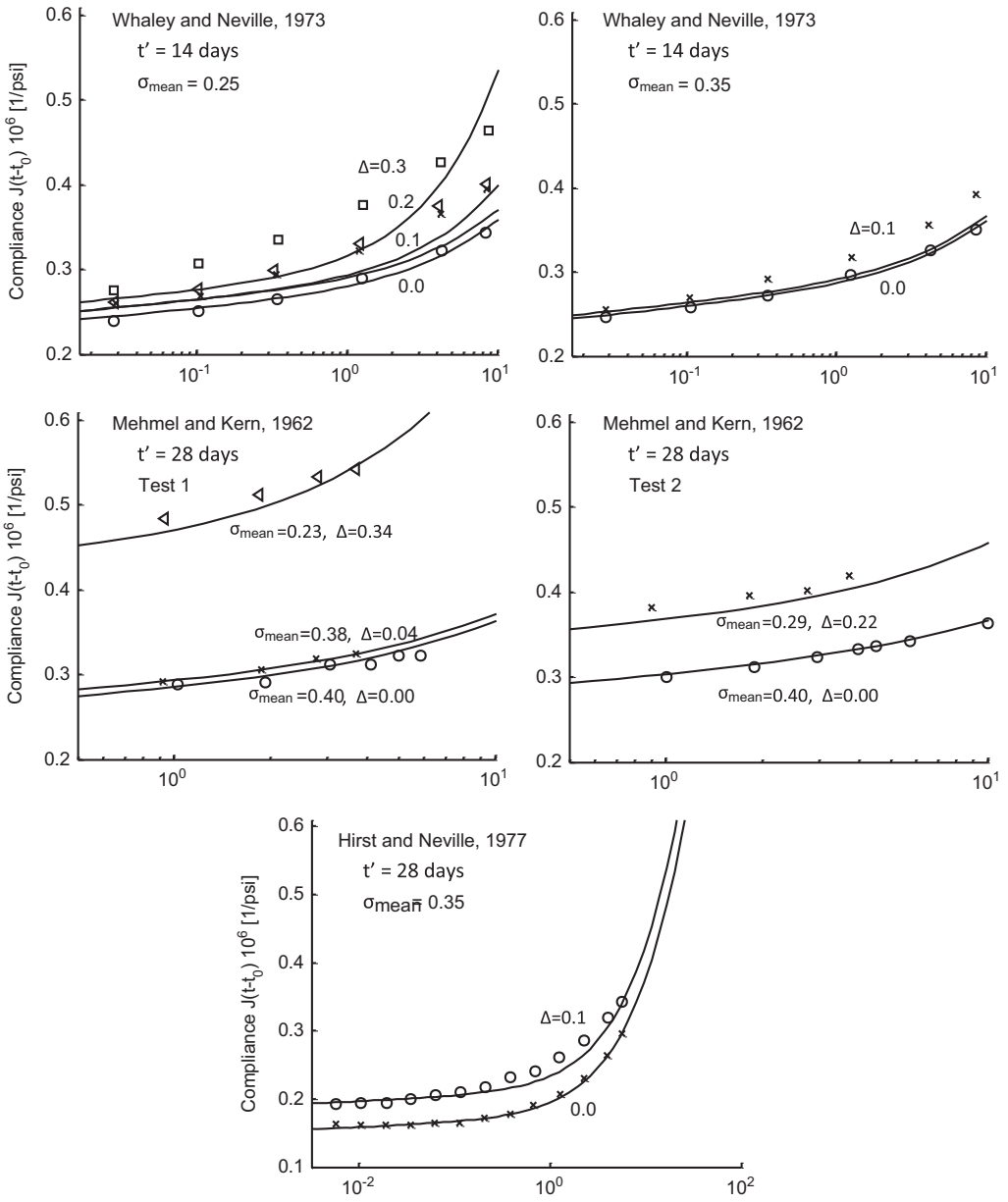

Fig. 4. Optimal fitting of test data by Whaley and Neville (1973), Kern and Mehmel (1962), and Hirst and Neville (1977).

et al., 2011a, 2011b, 2011c) and often develop more cracking than expected for a structure designed with a prestress that should be sufficient to avoid tensile stresses, according to the design code. When excessive deflections or cracking are discussed at conferences, one often hears an opinion putting the blame on cyclic creep without any supportive calculations.

Consider a simplified form of the cross section at pier of a box girder bridge, as shown in Fig. 6. For the sake of simplicity, we use the engineering theory of bending, with the cross sections remaining plane. The cross section dimensions and prestress level are designed so that the longitudinal normal stresses σ reach their allowable limits, $\sigma=-f_c (f_c>0)$ at bottom face of coordinate $z=-c_b (c_b>0)$ and $\sigma=f_t$ at top face of coordinate $z=c_t$ where coordinate z is measured from the cross section centroid and $c_b=h-c_t$, h=cross section depth. For sustained loading, the design code sets the allowable stress limits as $f_t=0$ and $f_c=0.4f'c$ where $f_c^{'}$ standard cylinder compressive strength of concrete.

According to the theory of bending, $-f_c=-(M_{DL}+Pe)c_b/I-P/A$ and $f_t=(M_{DL}+Pe)c_t/I-P/A$ where P, e=prestress force (positive for compression) and its eccentricity (positive if upwards); A, I=area and centroidal moment of inertia of cross section; $M_{DL}=M_D+M_L=$total bending moment (positive if causing compression on top), $M_D, M_L=$bending moments due to dead load (including self-weight) and to live load, representing the traffic load. By solving the foregoing two equations,

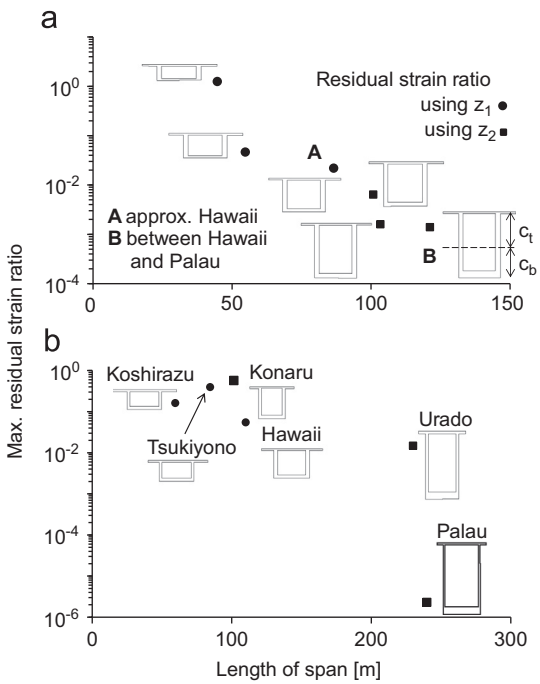

Fig. 5. Maximum residual strain ratios (Eq. 26) calculated for (a) a series of scaled cross sections design to allowable limits, and (b) a selection of actual bridge cross sections.

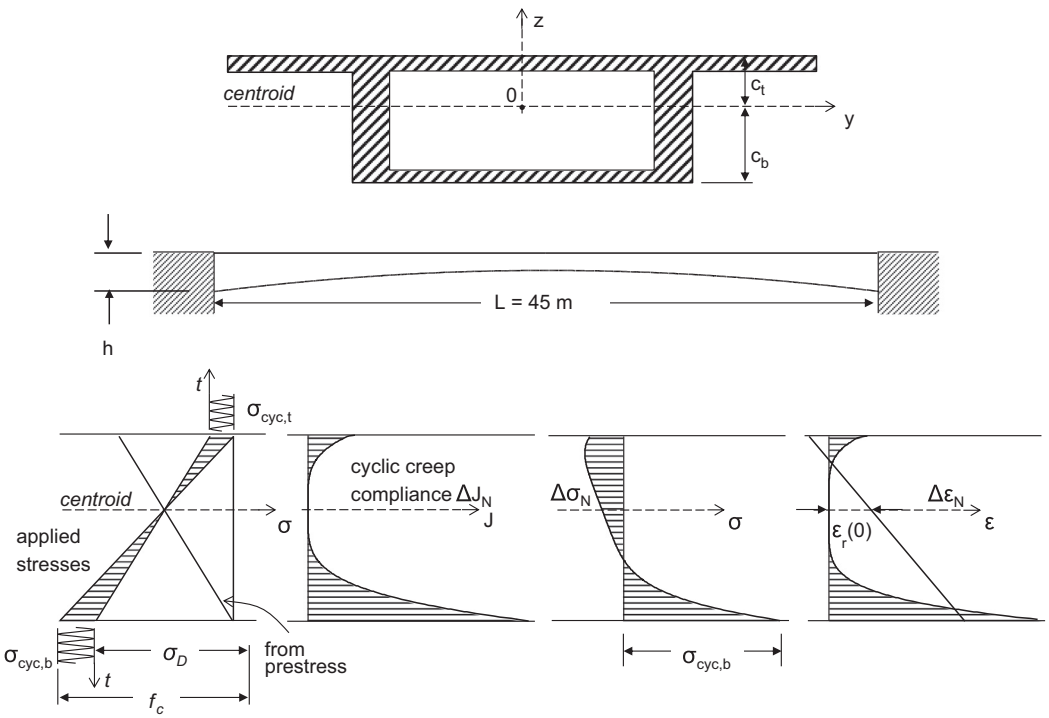

Fig. 6. An example of one of the scaled bridge cross sections at the pier for which the prestressing eccentricity and bridge span has been designed to reach allowable limits. Section profiles of the applied stresses due to dead load, cyclic live load and prestress, of the computed creep compliance, of the corresponding (free) cyclic creep strain, and of the resulting residual inelastic strain (or eigenstrain) required by cross section planarity.

one gets the P and M_{DL} values corresponding to the extreme allowable stresses:

$$P=\frac{A}{h}(f_c c_t - f_t c_b),\ M_{DL}=\left(f_c-\frac{P}{A}\right)\frac{I}{c_b}-Pe \tag{23}$$

The road traffic causes the bending moment to cycle between M_L and M_D+M_L (possible dynamic overloads are ignored). This produces the cyclic stress amplitude $\Delta\sigma$ and the static (or average) stress

$$\Delta\sigma=\frac{M_L z}{I},\ \sigma=\frac{-f_c z}{I}\left(M_D+\frac{M_L}{2}+Pe\right)-\frac{P}{A} \tag{24}$$

needed to calculate the inelastic cyclic strain from Eq. (14). Here $M_D+M_L/2=\overline{M}=$ average moment over the cycle. The use of the average is appropriate because it agrees with the symmetric periodic load fluctuations (Fig. 2a,d) used in the experiments and with the way Eq. (14) was calibrated from these experiments.

When, however, the load cycles are asymmetric as shown in Fig. 2b,c, the proper value of $\overline{M}$ is debatable since no such tests have been reported. If linear superposition of the load effects were applicable, then M_D would represent the time average of load over the cycle (shown by the horizontal dashed lines in Fig. 2). But since the dependence of cyclic creep on stress is highly nonlinear, the time shape of cycle is probably unimportant and mainly the extremes matter. Then the average value $\overline{M}=M_D+M_L/2$ may be used for all cycle shapes as seen in Fig. 2.

The inelastic strains (or eigenstrains) ε_N due to stress cycling, calculated for various z from Eq. (14) after substituting Eq. (24), do not satisfy the condition that the cross sections must remain planar. Therefore, self-equilibrated elastic residual strains ε_r must develop to enforce the planarity of cross sections, in the same way as it happens for shrinkage or thermal strains. The external complementary work of virtual normal force $\overline{N}$ and virtual bending moment $\overline{M}$ on residual normal strain ε_{r0} at the centroid and on residual curvature κ_r must be equal to the internal complementary virtual work of equilibrating virtual stresses $\overline{N}/A$ and $\overline{M}z/I$ on the corresponding cyclic inelastic strains $\varepsilon_{cyc}(z)$ over the cross section area A, i.e., $\overline{N}\varepsilon_{r0}=\int_A(\overline{N}/A)\varepsilon_{cyc}(z)\mathrm{d}A$ and $\overline{M}\kappa_r=\int_A(-\overline{M}z/I)\varepsilon_{cyc}(z)\mathrm{d}A$. These two complementary virtual work relations yield:

$$\varepsilon_{r0}=\frac{1}{A}\int_{c_b}^{c_t}\varepsilon_{cyc}(z)b(z)\,\mathrm{d}z,\ \kappa_r=-\frac{1}{I}\int_{c_b}^{c_t}\varepsilon_{cyc}(z)z\,b(z)\,\mathrm{d}z \tag{25}$$

where $\varepsilon_{cyc}(z)=$ free inelastic strain produced at level z by stress cycling (Eq. 14), $\mathrm{d}A=b(z)\mathrm{d}z$ and $b(z)=$combined width of cross section at level z. It follows that the residual strain and residual stress at any level z produced by cyclic creep is

$$\varepsilon_r(z)=\varepsilon_{cyc}(z)-(\varepsilon_{r0}-\kappa_r z),\ \sigma_{r,el}(z)=E\varepsilon_r(z) \tag{26}$$

where $E=$Young's modulus. The extreme values of $\varepsilon_r(z)$ and $\sigma_r(z)$ occur at either the top face, $z=c_t$, or the bottom face, $z=c_b$; $\sigma_{r,el}(z)$ represents the residual stresses that are produced by cyclic loading if the concrete remains elastic; their force and moment resultants are zero.

To evaluate the severity of cyclic creep effects, we will introduce two dimensionless measures, namely the inelastic residual strain ratio and the inelastic residual curvature ratio produced by load cycling:

$$\rho=\frac{\varepsilon_r^{max}}{f'_t/E},\ r=\frac{\kappa_r}{\kappa_{el}} \tag{27}$$

Here $\varepsilon_r^{max}=\max[\varepsilon_r(c_b),\varepsilon_r(c_t)]=$ maximum strain produced in the pier cross section by stress cycling (occurring at either top or bottom face); $E=$Young's modulus of concrete; $\kappa_{el}=$ maximum possible elastic curvature in the pier section, which is

$$\kappa_{el}=\frac{f_c+f_t}{Eh} \tag{28}$$

and corresponds to stresses at bottom and top faces being $-f_c$ and f_t.

Since we assumed the pier cross section to be designed so as to exhaust the allowable stress limits, the only variable is the amplitude of the live load, causing the cyclic stresses cross-hatched in Fig. 6 (left). Knowing the span and the cross section variation along the bridge, we can estimate the dead and live loads specified by the design code and the bending moments caused by them.

Fig. 6 shows the straight-line distribution of the maximum stress, varying between $-f_c$ and f_t, the distribution of dead load (or permanent) stress marked σ_D, and the line for the typical distribution of the prestress (whose time variation due to prestress losses is neglected). The second diagram to the right shows the distribution of the cyclic creep compliance, Δf_N (Eq. 20). The next diagram shows the distribution of cyclic creep strain, ε_{cyc}, calculated from Eq. (14), and the next and last diagram shows the distribution of the residual inelastic strain ε_r which results in damage and cracking.

Since we assume the pier cross section to be designed so as to exhaust the allowable stress limits, the only variable is the amplitude of the live load, the distribution of which is cross-hatched in Fig. 6 in the left-most diagram. Knowing the span and the cross section variation along the bridge, we can estimate the dead and live loads specified by the design code and the bending moments caused by them.

To appraise the cyclic creep effects in large prestressed segmental box girders, a collection of designs of six large-span bridges has been obtained through the courtesy of Y. Watanabe, Shimizu Construction Co., Tokyo (Japanese bridges Koshirazu, Tsukiyono, Konaru and Urado), of I. Robertson, University of Hawaii Manoa (North Halawa Valley Viaduct), and of G. Klein, WJE, Highland Park, Illinois (the ill-fated world-record bridge in Palau). The data on these bridges are used in Fig. 5–7 and for details of these bridges see (Bazant et al., 2012a, 2012b).

For the sake of easier comparability, it is assumed that, in all these bridges, the P and M_{DL} values were the maximum allowable for each cross section (Eq. 23). Based on the dimensions of each bridge, the live and dead loads (including the self-weight) are determined, and the bending moments at the pier are calculated assuming the girder to be rather flexible at

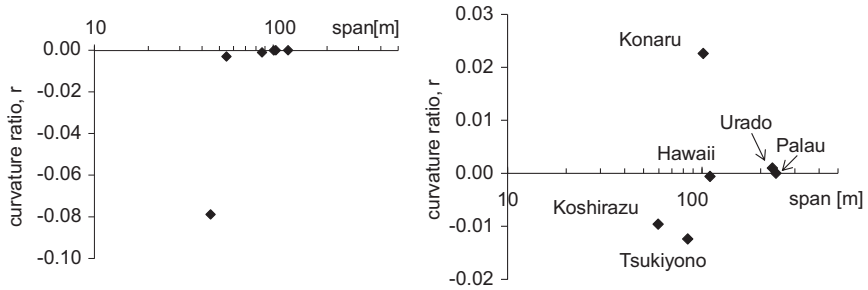

Fig. 7. The calculated curvature ratios for the actual bridge cross sections. The left figure shows systematically varying cross sections that reveal a transition from negative to positive curvature after a span of 80 m is reached. The right figures illustrate the values actual bridge cross sections may reach.

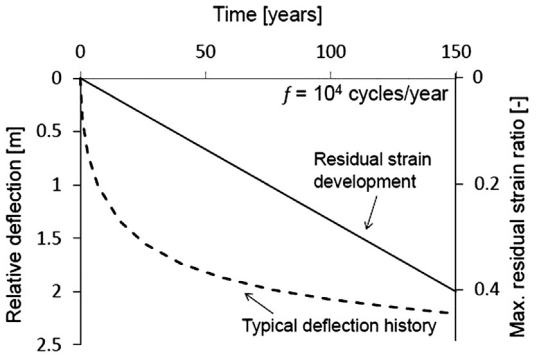

Fig. 8. Schematic comparison of the evolution of creep deflection and of the residual cyclic strain.

mid-span, in which case the moment at the pier is almost as large as it would be for a hinge at mid-span. The results for the residual strain ratio ρ and the cyclic creep curvature ratio r at $N=2$ million are plotted in Fig. 5 (bottom) and Fig. 7 (right).

The results for these bridges are rather scattered, which is obviously explained by variability in the cross section shapes. Therefore, another set of scaled bridge cross sections is generated by interpolating and extrapolating trend between the cross section of the Hawaii bridge (span 110 m) and of the KB bridge in Palau (span 241 m). A similar calculation procedure lead to the diagrams for ρ and r in Fig. 5 (top) and 7 (left).

Note that whereas the static long-time creep deflections grow in time logarithmically (Bazant et al., 2011a, 2012a), the cyclic creep deflections grow linearly (provided that the traffic load frequency and amplitude remain constant).

This property is verified by experiments and, theoretically, is a consequence of Paris law Eq. (11), which states that the crack extension is proportional to the number of cycles, N. Consequently, even if the cyclic creep effects are insignificant within the first 20 years of service, they may become significant, compared to creep, for a 100-year lifetime; see Fig. 8.

For the KB Bridge in Palau, the cyclic creep effects were virtually nil. Why? Partly because the traffic was light (low N), but mainly because this record-span bridge was totally dominated by self-weight. The bending moment due to traffic represented only about 2.5% of the total bending moment. Consequently, the ratio $\Delta\sigma/\sigma$ was unusually small, only about 0.025. Since the exponent, equal to 4, is high, one has $(\Delta\sigma/\sigma)^4 \approx 4\times 10^{-7}$. This explains why the cyclic creep contribution to curvature, deflection and cracking must have been, in this bridge, virtually zero. However, the high value, 4, of the exponent causes that a 20-fold increase of the ratio of traffic load to self-weight will increase the cyclic creep contribution about 10^5.

Much stronger effects of cyclic creep are seen in the plots of the curvature ratio r in Fig. 7. They reveal that, for spans between about 40 m and 120 m, the cyclic creep can produce significant tensile strains-times. These strains can approach or even exceed the maximum elastic strain at the top or bottom faces of the box girder. These strains get superposed on strains from differential shrinkage, drying creep and temperature, and obviously aggravate distributed tensile cracking, which may in turn lead to corrosion of reinforcement.

Other structures, such as those supporting large turbines or electric generators, can also suffer from surface tensile cracking caused by cyclic creep.

12. Conclusions

1. The mechanism of cyclic creep can be described by growth of preexisting micrometer-scale subcritical crack governed by Paris Law.
2. The relative increase of crack length must be considered small, in order to match the observed linear dependence of cyclic creep on the time-average stress.

3. The cyclic creep strain is obtained as the sum of openings of the microcracks calculated from the amplitude of the stress intensity factor, which itself is assumed to be proportional to the amplitude of the applied cyclic load.
4. Detailed derivation of the form of the cyclic creep law is possible mode I cracks, either tensile or (in the sense of crushing band) compressive. A general applicability of this law for various kinds of cracks under compressive loading can be justified by dimensional analysis and similitude arguments.
5. The derived cyclic creep law can fit the test data available in the literature quite well and has been calibrated by them. The data show that the Paris law exponent must be about 4. This observation is consistent with the recent finding that the Paris law exponent on the atomic scale must be 2 and that the exponent should roughly double during each scale transition, in this case from the nano-scale to the micrometer scale.
6. Exponent 4 is so high that cyclic creep deflections are enormously sensitive to the relative amplitude of the applied cyclic stress.
7. While the static creep deflections grow in time approximately logarithmically, the cyclic creep deflections grow linearly. This is a consequence of the Paris law. Consequently, even when the cyclic creep is unimportant for ten years of service, it may be important for hundred years of service.
8. For a broad time range, the long-term cyclic creep cannot be modelled as an acceleration of static creep.
9. Calculation examples indicate that, contrary to often voiced opinions, the cyclic creep effects are absolutely negligible for large-span prestressed segmental box girders, which are totally dominated by self weight. In particular, the cyclic creep could have played no role in the excessive deflections of the ill-fated world-record KB Bridge in Palau. For small spans (<40 m), the cyclic creep deflections are not negligible but it does not matter since the static creep in such bridges causes upward deflections.
10. Cyclic creeps can produce major tensile strains in small and medium span prestressed bridges, and thus contribute significantly to their cracking and corrosion.

Acknowledgments

Financial support from the U.S. Department of Transportation, provided through Grant 20778 from the Infrastructure Technology Institute of Northwestern University, is gratefully appreciated. Further support was provided under U.S. National Foundation Grant CMMI-1153494 to Northwestern University. Thanks are due to Prof. Milan Jirásek and Milan Havlásek of the Czech Technical University in Prague for stimulating critical comments and help in bridge studies, respectively.

References

ACI Committee 209, 1972. Prediction of creep, shrinkage and temperature effects in concrete structures. *ACI-SP27, Designing for Effects of Creep, Shrinkage and Temperature*, Detroit, pp. 51–93.
ACI Committee 209 (2008). Guide for Modeling and Calculating Shrinkage and Creep in Hardened Concrete. ACI Report 209.2R-08, Farmington Hills.
Ashby, M.F., Hallam, S.D., 1986. The failure of brittle solids containing small cracks under compressive stress states. Acta Metall. Mat. 34 (3), 497–510.
Barenblatt, G.I., 2003. Scaling. Cambridge University Press, Cambridge, UK.
Barenblatt, G.I., 1979. Similarity, Self-Similarity and Intermediate Asymptotics. Consultants Bureau, New York, NY.
Batson, G., et. al., 1972. J. Am. Conc. Res. 69, 673.
Bazant, Z.P., 1968a. On causes of excessive long-time deflections of prestressed concrete bridges. Creep under repeated live load. In: Czech, Inženýrské Stavby, 16, pp. 317–320.
Bazant, Z.P., 1968b. Langzeitige Durchbiegungen von Spannbetonbrücken infolge des Schwingkriechens unter Verkehrslasten. Long-time deflections of pre-stressed concrete bridges due to cyclic creep under traffic loads, Beton und Stahlbetonbau 63, 282–285.
Bazant, Z.P., Baweja, S., 2000. Creep and shrinkage prediction model for analysis and design of concrete structures: Model B3. Adam Neville Symposium: Creep and Shrinkage—Structural Design Effects, ACI SP–194, A. Al-Manaseer, ed., pp. 1–83 (update of 1995 RILEM Recommendation).
Bazant, Z.P., Baweja, S., 1995. Creep and shrinkage prediction model for analysis and design of concrete structures: Model B3 (RILEM Recommendation) Materials and Structures, 28, pp. 357–367 (Errata, Vol. 29, p. 126).
Bazant, Z.P., Hubler, M.H., Yu, Q., 2011a. Pervasiveness of excessive deflections of segmental bridges: wake-up call for creep. ACI Struc. J. 108 (6), 766–774.
Bazant, Z.P., Hubler, M.H., Yu, Q., 2011b. Excessive creep deflections: an awakening. ACI Concr. Int. 33 (8), 44–46.
Bazant, Z.P., Yu, Q., Hubler, M., Křístek, V., Bittnar, Z., 2011. Wake-up call for creep, myth about size effect and black holes in safety: what to improve in *fib* model code draft. In: *Concrete Engineering for Excellence and Efficiency* (Proceedings of the *fib* Symp. Prague, Topic 3 Keynote Lecture) (ISBN 978-87158-26-7), pp. 731–746.
Bazant, Z.P., Kim, J.-K., Panula, L., 1992. Improved prediction model for time-dependent deformations of concrete: Part 5–Cyclic load and cyclic humidity. Mater. Struc. (RILEM, Paris) 25 (147), 163–169.
Bazant, Z.P., Le, J.-L., 2009. Nano- mechanics based modeling of lifetime distribution of quasi-brittle structures. Eng. Failure Anal. 16, 2521–2529.
Bazant, Z.P., Panula, L., 1979. Practical prediction of time-dependent deformations of concrete. Part VI: cyclic creep, nonlinearity and statistical scatter. Mater. Struc. (RILEM, Paris) 12, 175–183.
Baănt, Z.P., Schell, W.F., 1993. Fatigue fracture of high-strength concrete and size effect. ACI Mater. J. 90 (5), 472–478.
Bazant, Z.P., Xiang, Y., 1997. Size effect in compression fracture: splitting crack band propagation. J. Eng. Mech. ASCE 123 (2), 162–172.
Bazant, Z.P., Xu, K., 1991. Size effect in fatigue fracture of concrete. ACI Mater. J. 88 (4), 390–399.
Bazant, Z.P., Yu, Q., Li, G.-H., 2012a. Excessive long-time deflections of prestressed box girders: I. record-span bridge in Palau and other paradigms. J. Struc. Eng. ASCE 138 (6), 676–686.
Bazant, Z.P., Yu, Q., Li, G.-H., 2012b. Excessive long-time deflections of prestressed box girders: II. numerical analysis and lessons learned. J. Struc. Eng. ASCE 138 (6), 687–696.
Bechyně, S., 1959. Concrete Construction. I. Concrete Technology, SNTL, Prague, pp. 122–136 (in Czech).
Bennett, E.W., Muir, St.J., 1967. Magazine of Concrete Research 19, 113.
Brooks, J.J., Forsyth, P., 1986. Influence of frequency of cyclic load on creep of concrete. Mag. Concr. Res. 38 (136), 139–150.

Buckingham, E., 1914. On physically similar systems: illustrations of the use of dimensional equations. Phys. Rev. 4, 345–376.
Castigliano, A., 1873. Théorie de l équilibre des systèmes élastiques (Engineering Degree Thesis). Politecnico di Torino, Turin.
Flügge, W. (Ed.), 1962. Handbook of Engineering Mechanics. McGraw-Hill, New York. (sections 26–18, 27–3, 33–21).
Eliáš, J., Le, J.-L., 2012. Modeling of mode-I fatigue crack growth in quasibrittle structures under cyclic compression. Engrg. Fracture Mech., 96, 26–36, ISSN 0013-7944, http://dx.doi.org/10.1016/j.engfracmech.2012.06.019.
Fairhurst, C., Comet, F., 1981. Rock fracture and fragmentation. In: Einstein, H.H. (Ed.), Rock Mechanics: from Research to Application. Proceedings of the U.S. Symposium on Rock Mechanics. MIT Press, Cambridge, MA, pp. 21–46.
FIB, 1999. Structural Concrete: Textbook on Behaviour, Design and Performance, Updated Knowledge of the CEB/FIP Model Code 1990. Bulletin No. 2, Fédération internationale du béton (FIB), Lausanne, vol. 1, pp. 35–52.
Gaede, K., 1962. Versuche über die Festigkeit und die Verformungen von Beton bei Druck-Schwellbeansruchung. Deutscher Ausschußfür Stahlbeton, Heft 144, W. Ernst & Sohn, Berlin.
Gao, L., Hsu, C.-T.T., 1998. Fatigue of concrete under compression cyclic loading. ACI Mater. J. 95 (5), 575–579.
Gardner, N.J., 2000. Design provisions of shrinkage and creep of concrete. In: AlManaseer, A. (Ed.), Adam Neville Symposium: Creep and Shrinkage – Structural Design Effect, ACI SP-194, pp. 101–104.
Gardner, N.J., Lockman, M.J., 2001. Design provisions for drying shrinkage and creep of normal strength. ACI Mater. J. 98 (March–April (2)), 159–167.
Garrett, G.G., Jennings, H.M., Tait, R.B., 1979. The fatigue hardening behavior of cement-based materials. J. Mat. Sci. 14, 296–306.
Gvozdev, A.A., 1966. Polzuchest' betona (concrete creep), Trudy Vsesoyuznogo Sjezda po Teor. i Prikl. Mekhanike, Mekhanika Tverdogo Tela, Nauka, Moscow, pp. 137–152.
Hellesland, J., Green, R., 1971. Sustained and cyclic loading of concrete columns. Proc. ASCE 97 (ST4), 1113–1128.
Hirst, G.A., Neville, A.M., 1977. Activation energy of concrete under short-term static and cyclic stresses. Mag. Concr. Res. 29 (98), 13–18.
Horii, H., Nemat-Nasser, S., 1982. Compression induced nonplanar crack extension with application to splitting, exfoliation and rockburst. J. Geophys. Res. 87, 6806–6821.
Hsu, T.C., 1981. Fatigue of plain concrete. ACI J. 78 (4), 292–305.
Ingraffea, A.R., 1977. Discrete Fracture Propagation in Rock: Laboratory Tests and Finite Element Analysis (Ph.D. dissertation). University of Colorado, Boulder.
Kachanov, M., 1982. A microcrack model of rock inelasticity-part I. Frictional sliding on microcracks. Mech. Mat. 1, 19–41.
Kanninen, M.F., Popelar, C.H., 1985. Advanced Fracture Mechanics. Oxford University Press, New York.
Kemeny, 1.M., Cook, N.G.W., 1987. Crack models for the failure of rock under compression. in: Desai et al., C.S. (Eds.), Proceedings of the 2nd International Can. on Constitutive Laws for Engineering Materials, Elsevier Science Publishing Co. Inc., New York, N.Y., 2, 879–887.
Kern, E., Mehmel, A., 1962. Elastische und plastische Stauchungen von Beton infolge Druckschwell- und Standbelastung. Deutscher Ausschuß für Stahlbeton, Heft 153, W. Ernst & Sohn, Berlin.
Le, J.-L., Bazant, Z.P., 2011. Unified nano-mechanics based probabilistic theory of quasibrittle and brittle structures: II. fatigue crack growth, lifetime and scaling. J. Mech. Phys. Solids 59, 1322–1337.
Le Camus, B., 1946. Recherches expérimentale sur la déformation du béton et du béton armé. Cahiers de la recherche des lab. du bât. et des travaux publ., Circ. ITB (Ser. F, No. 27), Paris.
L'Hermite, R., 1961. Que savons nous de la déformation plastique et du fluage du béton? Annales I.T.B.T.P. IX, Np. 117, Paris.
L'Hermite, R., 1961. Les déformations du béton. Cahiers de la recherche, No. 12, I.T.B.T.P., Eyrolles, Paris (Fig. 16, pp. 65–67).
Maekawa, K., El-Kashif, K.F., Cyclic cumulative damaging of reinforced concrete in post-peak regions. J. Adv. Conc. Tech. 2 (2), 257–271.
Mal'mejster, A.K., 1957. Uprugost' i neuprugost' betona, (Elasticity and Inelasticity of Concrete). Izdatel'stvo A.N. Latvian SSR, Riga.
Murdock, G.M., 1965. A critical review of research on fatigure of plain concrete. Univ. Illinois Bull. Engrg. Exp. Station 62 (February), 475.
Neville, A.M., Hirst, G.A., 1978. Mechanism of cyclic creep of concrete. In: Douglas McHenry International Symposium on Concrete and Concrete Structures ACI SP-55, pp. 83–101.
Nordby, G.M., 1967. Fatigue of concrete—a review of research. J. Am. Concr. Inst. 30 (2), 191–219.
Pandolfi, A., Taliercio, A., 1998. Bounding surface models applied to fatigue of plain concrete. J. Eng. Mech. (May), 556–564.
Paris, P.C., Erdogan, F., 1963. Critical analysis of propagation laws. J. Basic Eng. 85, 528–534.
Sammis, C.G., Ashby, M.F., 1986. The failure of brittle porous solids under compressive stress state. Acta Metall. Mat. 34 (3), 511–526.
Schulson, E.M., Nickolayev, O.Y., 1995. Failure of columnar saline ice under biaxial compression: failure envelopes and the brittle to-ductile transition. J. Geophys. Res. 100 (B11), 22383–22400.
Suresh, S., 1998. Fatigue of Materials. Cambridge University Press, Cambridge, U.K.193.
Suresh, S., Tschegg, E.K., Brockenbrough, J.R., 1989. Crack growth in cementitious composites under cyclic compressive loads. Cem. Concr. Res. 19, 827–833.
Tada, H., Paris, P.C., Irwin, G.R., 1973. The Stress Analysis of Cracks Handbook. Del Research Corporation, Hellerton, PA.
Vashy, A., 1892. Sur les lois de similitude en physique. Ann. télegraphiques 19, 25–28.
Whaley, C.P., Neville, A.M., 1973. Non-elastic deformation of concrete under cyclic compression. Mag. Concr. Res. 25 (84), 145–154.
Wittmann, V.F., 1971. Kriechverformung des Betons unter statischer und unter dynamischer Belastung. Rheol. Acta 10, 422–428.